

**HADRONIC DIFFRACTION: WHERE DO WE STAND?\***

Konstantin Goulianos

*The Rockefeller University, 1230 York Avenue, New York, NY 10021, USA*

## Abstract

Experimental results on hadronic soft and hard diffractive processes are reviewed with emphasis on aspects of the data that point to the underlying QCD mechanism for diffraction. Diffractive differential cross sections are shown to be factorized into two terms, one representing the total cross section at the reduced energy, corresponding to the rapidity region(s) in which there is particle production, and another interpreted as the probability of formation of the rapidity gap(s) characterizing diffraction. By (re)normalizing the term of gap formation probability to unity, cross sections for single, central, and multiple rapidity gap soft diffraction, as well as structure functions for hard diffraction processes, are obtained from the underlying inclusive parton distribution functions. A unified partonic picture emerges, in which diffraction appears to be mediated by the exchange of low- $x$  partons subject to color constraints.

---

\* To appear in: *Proc. Les Rencontres de Physique de la Vallée d'Aoste*, La Thuile, Aosta Valley, Italy, February 29 - March 6, 2004.

## 1 Introduction

Hadronic diffraction has traditionally been treated in the framework of Regge theory <sup>1)</sup>. In this approach, the key player mediating diffractive processes is the Pomeron ( $\mathbb{P}$ ) *Regge trajectory*, presumed to be delineated by a “family” of particles carrying the quantum numbers of the vacuum. Although no particles were known (and have yet to be found!) to belong to this family, the Pomeron trajectory was introduced in the 1970s to account for the observations that the  $K^+p$  cross section was increasing with energy at the Serpukov 70 GeV proton synchrotron, and the elastic and total  $pp$  cross sections, which were falling with increasing energy, started to flatten out and then increase as larger collision energies became available at the CERN Intersecting Storage Ring (ISR)  $pp$  collider.

Regge theory worked reasonably well in describing elastic, diffractive and total hadronic cross sections at energies up to  $\sqrt{s} \sim 50$  GeV, spanning the range of Serpukov, Fermilab, and ISR energies. All processes could be accommodated in a simple Pomeron pole approach. This success was documented, among other places, in a 1983 Physics Reports article by this author <sup>2)</sup>. Results from a Rockefeller University experiment on photon dissociation on hydrogen published in 1985 <sup>3)</sup> were also well described in this approach.

The early success of Regge theory was precarious. The theory was known to asymptotically violate unitarity, as the  $\sim s^\epsilon$  power law increase of total cross sections would eventually exceed the Froissart bound of  $\sigma_T < C \cdot \ln^2 s$  based on analyticity and unitarity. But the confrontation with unitarity came far earlier than what would be considered asymptopia by Froissart bound considerations. As collision energies climbed upwards in the 1980s to reach  $\sqrt{s} = 630$  GeV at the CERN  $S\bar{p}pS$  collider and  $\sqrt{s} = 1800$  GeV at the Fermilab Tevatron  $\bar{p}p$  collider, diffraction dissociation could no longer be accommodated within a factorizable Regge pole framework in which the Pomeron exchange contribution to total, elastic, and single diffractive  $pp$  cross sections is given by

$$\sigma^{tot}(s) = \beta_{\mathbb{P}pp}^2(0) \left( \frac{s}{s_0} \right)^{\alpha_{\mathbb{P}}(0)-1} \quad (1)$$

$$\frac{d\sigma^{el}}{dt} = \frac{\beta_{\mathbb{P}pp}^4(t)}{16\pi} \left( \frac{s}{s_0} \right)^{2[\alpha_{\mathbb{P}}(t)-1]} \quad (2)$$

$$\frac{d^2\sigma_{sd}}{d\xi dt} = \underbrace{\frac{\beta_{\mathbb{P}pp}^2(t)}{16\pi} \xi^{1-2\alpha_{\mathbb{P}}(t)}}_{f_{\mathbb{P}/p}(\xi,t)} \left[ \beta_{\mathbb{P}pp}(0) g(t) \left( \frac{s'}{s_0} \right)^{\alpha_{\mathbb{P}}(0)-1} \right] \quad (3)$$

where  $\alpha_{\mathbb{P}}(t) = \alpha_{\mathbb{P}}(0) + \alpha' t = (1 + \epsilon) + \alpha' t$  is the Pomeron trajectory,  $\beta_{\mathbb{P}pp}(t)$  the coupling of the Pomeron to the proton,  $g(t)$  the  $\mathbb{P}\mathbb{P}\mathbb{P}$  coupling,  $s' = M^2$  the  $\mathbb{P} - p$  center of mass energy squared,  $\xi = 1 - x_F = s'/s = M^2/s$  the fraction of the momentum of the proton carried by the Pomeron, and  $s_0$  an energy scale parameter traditionally set to the hadron mass scale of 1 GeV<sup>2</sup>.

The single diffractive cross section, Eq. (3), factorizes into two terms, the one in square brackets, which can be viewed as the  $\mathbb{P}$ - $p$  total cross section, and the other labeled  $f_{\mathbb{P}/p}(\xi, t)$ , which may be interpreted as the Pomeron flux emitted by the diffracted proton. In 1985, Ingelman and Schlein (IS) proposed that the Pomeron may have partonic structure and, assuming various forms for its structure, predicted diffractive dijet production rates by replacing the  $\mathbb{P}$ - $p$  total cross section in Eq. (3) by the parton level cross section. When later the UA8 Collaboration discovered and characterized diffractive dijet production in  $\bar{p}p$  collisions at  $\sqrt{s} = 630$  GeV <sup>5)</sup>, the reported measured rate was severely suppressed relative to that expected from the IS model using a Pomeron flux based on Regge theory and factorization. However, it was not clear at that time whether this discrepancy represented a breakdown of factorization or failure of the IS model.

The first clear experimental evidence for a breakdown of factorization in Regge theory was reported by the CDF Collaboration in 1994 <sup>6)</sup>. CDF measured the single diffractive cross section in  $\bar{p}p$  collisions at  $\sqrt{s} = 546$  and 1800 GeV and found a suppression factor of about an order of magnitude at  $\sqrt{s} = 1800$  GeV relative to predictions based on extrapolations from  $\sqrt{s} \sim 20$  GeV. The suppression factor at  $\sqrt{s} = 546$  GeV was  $\sim 5$ , approximately equal to that reported by UA8 for hard diffraction at  $\sqrt{s} = 630$  GeV. The

near equality of the suppression in soft and hard diffraction provided the clue that led to the development by this author of a *renormalization* procedure for single diffraction, which was later extended to central and multigap diffractive processes, as described in the following sections.

## 2 Renormalization and scaling in single diffraction

The breakdown of factorization in Regge theory was traced to the energy dependence of  $\sigma_{sd}^{tot}(s) \sim s^{2\epsilon}$ , which is faster than that of  $\sigma^{tot}(s) \sim s^\epsilon$ , so that as  $s$  increases unitarity would have to be violated if factorization holds. This is reflected in an explicit  $s$ -dependence in  $d\sigma_{sd}(M^2)/dM^2$ :

$$\text{Regge theory: } d\sigma_{sd}(M^2)/dM^2 \sim s^{2\epsilon}/(M^2)^{1+\epsilon} \quad (4)$$

In a paper first presented by this author in 1995 at La Thuile <sup>7)</sup> and Blois <sup>8)</sup> and later published in Physics Letters <sup>9)</sup>, it was shown that unitarization could be achieved, and the factorization breakdown in single diffraction fully accounted for, by interpreting the Pomeron flux of Eq. (3) as a probability density and *renormalizing* its integral over  $\xi$  and  $t$  to unity,

$$\text{renormalization: } f_{\mathbb{P}/p}(\xi, t) \Rightarrow N_s^{-1} \cdot f_{\mathbb{P}/p}(\xi, t) \quad (5)$$

$$\text{where } N_s \equiv \int_{\xi(\min)}^{\xi(\max)} d\xi \int_{t=0}^{-\infty} dt f_{\mathbb{P}/p}(\xi, t) \sim s^{2\epsilon}$$

where  $\xi(\min) = M_0^2/s$  (with  $M_0^2 = 1.4 \text{ GeV}^2$ : effective threshold for diffraction dissociation), and  $\xi(\max) = 0.1$ . The energy dependence of  $N_s^{-1}$ , introduced by renormalization, removes the explicit  $s$ -dependence from  $\sigma_{sd}^{tot}$ , thereby ensuring unitarization. In Fig. 1,  $\sigma_{sd}^{tot}(s)$  is compared with Regge predictions using the standard or renormalized Pomeron flux. The renormalized prediction is in excellent agreement with the data.

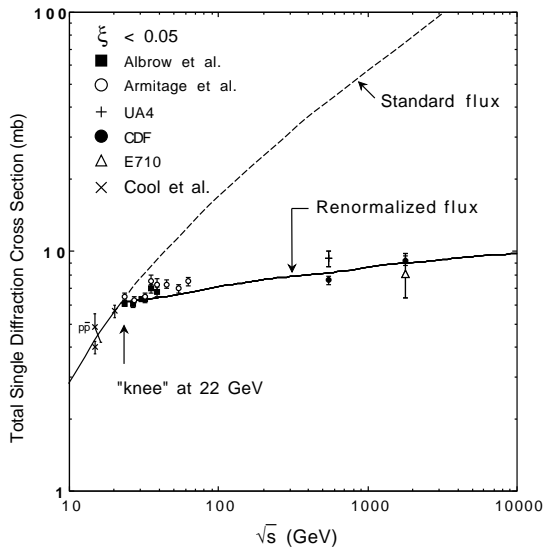


Figure 1: Total  $pp/\bar{p}p$  single diffraction dissociation cross section data (both  $\bar{p}$  and  $p$  sides) for  $\xi < 0.05$  compared with predictions based on the standard and the renormalized Pomeron flux [from Ref. <sup>9)</sup>].

It should be noted that the elastic and total cross sections are not affected by this procedure. One way to achieve unitarization in these cases is by using the eikonal approach, as reported by Covolan, Montanha and this author<sup>10)</sup>. As shown in Fig. 2, excellent agreement is obtained between elastic and total cross section data and predictions based on Regge theory and eikonalization.

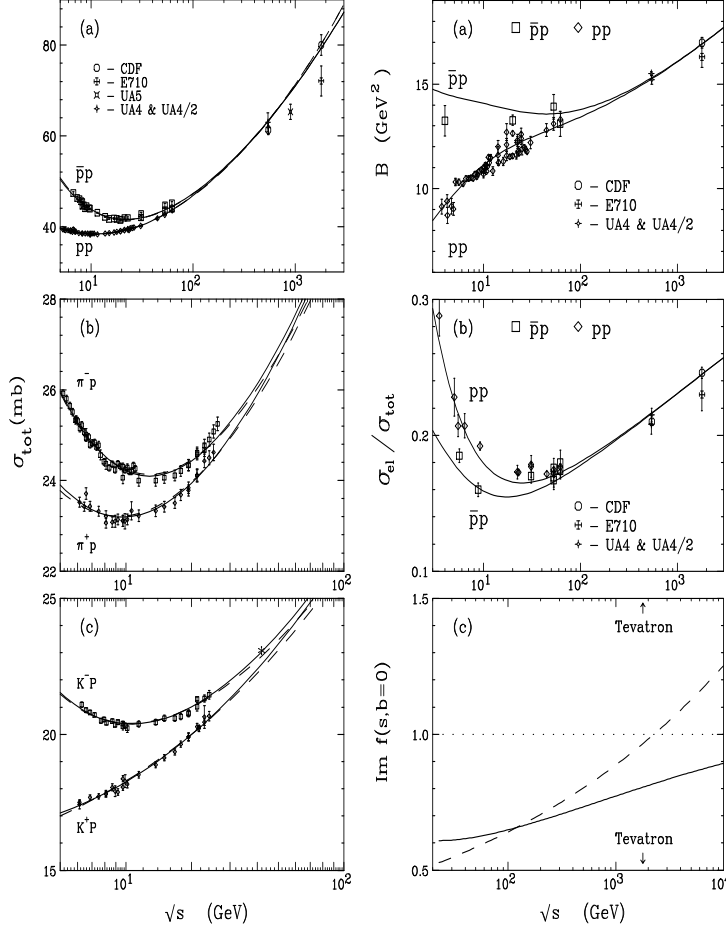


Figure 2: Fits to total cross section and elastic scattering data. The dashed lines are Born level Regge fits, and the solid lines are fits after eikonalization of the elastic scattering amplitude [from Ref. <sup>10)</sup>].

An important aspect of renormalization is that it leads to a scaling behavior, whereby  $d\sigma_{sd}(M^2)/dM^2$  has no explicit  $s$ -dependence:

$$M^2\text{-scaling: } d\sigma_{sd}(M^2)/dM^2 \sim 1/(M^2)^{1+\epsilon} \quad (6)$$

This ‘scaling law’ was demonstrated for *differential* soft single diffractive cross sections in a paper by Montanha and this author<sup>11)</sup>, in which renormalization was exploited to achieve a fit to all  $pp$  and  $\bar{p}p$  cross section data with only one free parameter - see also Refs. 12, 13, 14, 15, 16) for scaling behavior in hard diffraction. Figure 3 shows a comparison between data and the standard Regge and renormalization predictions for  $d\sigma_{sd}(M^2)/dM^2$ . The renormalization prediction provides an excellent fit to the data over five orders of magnitude.

As discussed below,  $M^2$ -scaling represents a general behavior extending to central and multigap diffractive processes.

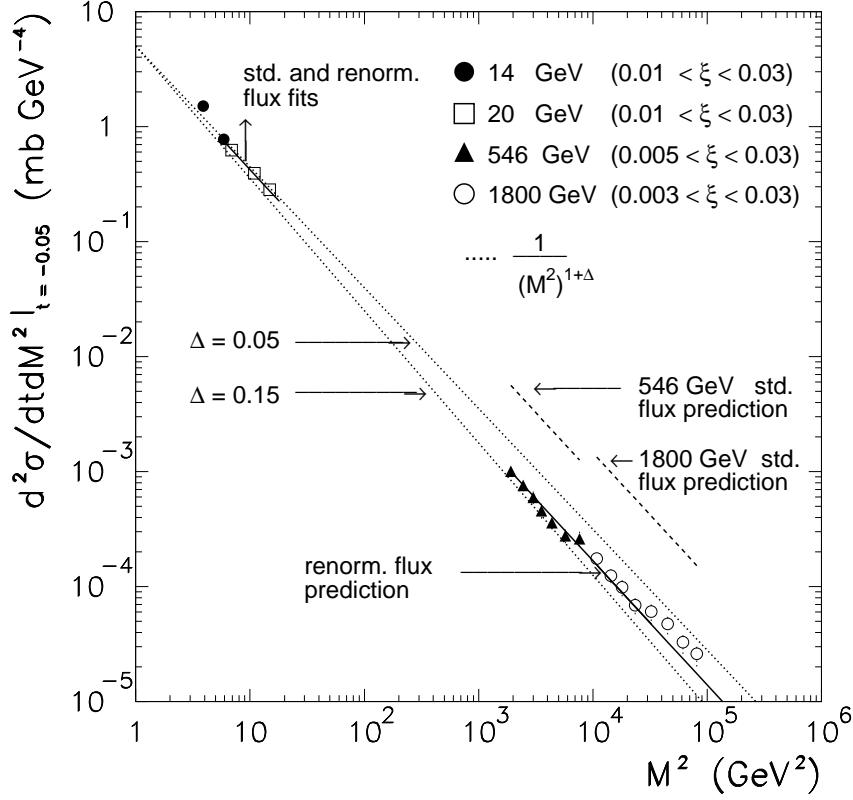


Figure 3: Cross sections  $d^2\sigma_{sd}/dM^2 dt$  for  $p + p(\bar{p}) \rightarrow p(\bar{p}) + X$  at  $t = -0.05 \text{ GeV}^2$  and  $\sqrt{s} = 14, 20, 546$  and  $1800 \text{ GeV}$ . Standard (renormalized) flux predictions are shown as dashed (solid) lines. At  $\sqrt{s}=14$  and  $20 \text{ GeV}$ , the fits using the standard and renormalized fluxes coincide [from Ref. <sup>11</sup>].

### 3 Central rapidity gaps: double diffraction

Double diffraction dissociation is the process in which both colliding hadrons dissociate leading to events with a central rapidity gap<sup>1</sup> (see Fig. 4).

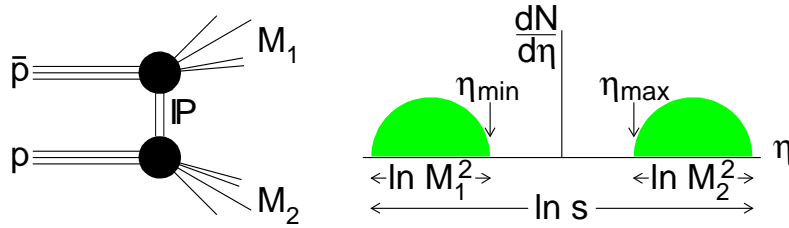


Figure 4: Schematic diagram and event topology of  $\bar{p}p$  double diffraction dissociation; the shaded areas represent regions of particle production [from Ref. <sup>18</sup>].

In Regge theory, the DD cross section is given by <sup>2)</sup>

$$\frac{d^3\sigma^{dd}}{dt dM_1^2 dM_2^2} = \frac{d^2\sigma_1^{sd}}{dt dM_1^2} \frac{d^2\sigma_2^{sd}}{dt dM_2^2} / \frac{d\sigma^{el}}{dt} = \frac{[\kappa\beta_1(0)\beta_2(0)]^2}{16\pi} \frac{s^{2\epsilon} e^{b_{dd}t}}{(M_1^2 M_2^2)^{1+2\epsilon}} \quad (7)$$

<sup>1</sup>We use rapidity,  $y \equiv \frac{1}{2} \ln \frac{E+p_L}{E-p_L}$ , and pseudorapidity,  $\eta \equiv -\ln(\tan \frac{\theta}{2})$ , interchangeably, as they are approximately equal in the kinematic range of interest.

where  $b_{dd} = 2\alpha' \ln(ss_0/M_1^2 M_2^2)$ . Since there is no term in this formula that can be identified as Pomeron flux, it was not immediately clear how renormalization should be applied in DD. The procedure employed in Ref. 9) is, in hindsight, incorrect. The clue to the correct procedure is embedded in a 1998 paper by this author<sup>17)</sup>, in which the SD cross section is expressed in terms of the rapidity gap variable,  $\Delta\eta$ , in place of  $\xi$  or  $M^2$ . These variables are related by

$$\Delta\eta = \ln \frac{s}{M^2} = -\ln \xi \quad (8)$$

Using rapidity gap variables, the SD and DD cross sections take the forms

$$\frac{d^2\sigma_{sd}}{dtd\Delta\eta} = \left[ \frac{\beta^2(t)}{16\pi} e^{2[\alpha(t)-1]\Delta\eta} \right] \cdot \kappa \left[ \beta^2(0) \left( \frac{s'}{s_0} \right)^\epsilon \right] \quad (9)$$

$$\frac{d^3\sigma_{dd}}{dtd\Delta\eta d\eta_c} = \left[ \frac{\kappa\beta^2(0)}{16\pi} e^{2[\alpha(t)-1]\Delta\eta} \right] \cdot \kappa \left[ \beta^2(0) \left( \frac{s'}{s_0} \right)^\epsilon \right] \quad (10)$$

where  $\kappa \equiv g_{\mathbb{P}\mathbb{P}\mathbb{P}}/\beta_{\mathbb{P}\mathbb{P}\mathbb{P}}$ ,  $\eta_c$  the center of the rapidity gap, and  $s'$  the reduced collision energy squared, defined by

$$\text{reduced energy: } \ln \frac{s'}{s_0} = \sum_i \ln \frac{M_i^2}{s_0} \Rightarrow \frac{s'}{s_0} = \exp \left[ \sum_i \Delta\eta'_i \right] \quad (11)$$

The expressions for the SD and DD cross sections are strikingly similar, except that in DD the gap is not “tied” to the (anti)proton and therefore  $\eta_c$  is treated as an independent variable. The two factors in brackets on the right hand side are identified as the rapidity gap probability and the reduced energy total cross section, respectively. In both SD and DD, the gap probability has the same  $\Delta\eta$  dependence and its integral over all phase space is  $\sim s^{2\epsilon}$ :

$$P_{gap}(\Delta\eta) \sim e^{2\epsilon\Delta\eta} \Rightarrow \int_{\Delta\eta(\min)}^{\ln s} P_{gap}(\Delta\eta) d\Delta\eta \sim s^{2\epsilon} \quad (12)$$

Thus, renormalization cancels the  $s^{2\epsilon}$  factor in Eq. (7), ensuring  $M^2$ -scaling and predicting similar suppression factors for SD and DD. In 2001, CDF reported results verifying this prediction<sup>18)</sup>. Fig. 5 shows a comparison between DD total cross sections versus  $s$  and predictions based on Regge theory with and without renormalization. The renormalized prediction is in excellent agreement with the data.

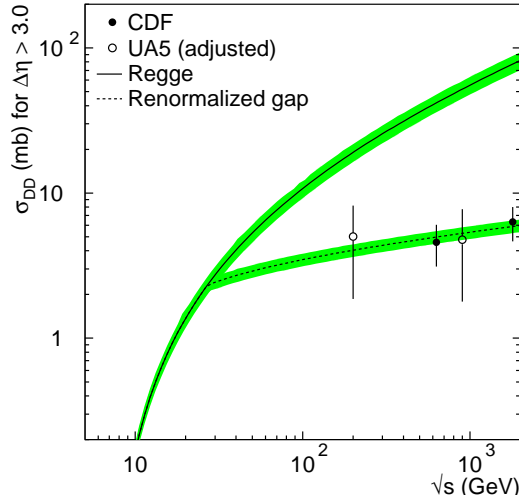


Figure 5: *The total  $\bar{p}p$  double diffractive cross section versus  $s$  [from Ref. 18)].*

#### 4 Multigap diffraction

Following the success of the renormalized gap probability model in correctly predicting double diffraction dissociation, the next challenge was to understand events with multiple rapidity gaps. The classical example of a two-gap process is double Pomeron exchange,  $\bar{p} + p \rightarrow \bar{p} + (gap) + X + (gap) + p$ , where the  $\bar{p}$  and  $p$  are scattered quasi-elastically and a central system  $X$  of mass  $M$  is produced separated from the outgoing nucleons by large rapidity gaps (see Fig. 6).

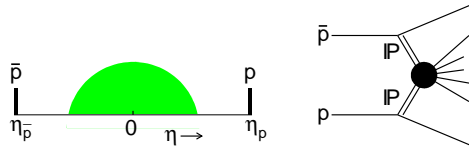


Figure 6: *DPE: Double Pomeron Exchange*

In Regge theory, the expression for DPE analogous to that of Eq. (3) for SD is

$$\frac{d^4\sigma}{dt_{\bar{p}}dt_p d\xi_{\bar{p}}d\xi_p} = f_{\mathbb{P}/\bar{p}}(\xi_{\bar{p}}, t_{\bar{p}}) \cdot f_{\mathbb{P}/p}(\xi_p, t_p) \cdot \kappa^2 \left[ \beta^2(0) \left( \frac{s'}{s_0} \right)^\epsilon \right] \quad (13)$$

When the renormalization model was proposed<sup>9)</sup>, it was presumed that both the  $\bar{p}$  and  $p$  Pomeron fluxes ought to be renormalized to unity. This leads to a DPE cross section which is doubly suppressed as  $\sigma_{sd}$ . After generalizing the Pomeron flux model it became clear that the gap probability depends on the sum of the two gaps and therefore there should be no additional suppression due to the second gap. In 2001, a procedure for multigap renormalization was proposed by this author<sup>19, 20, 21)</sup> on the basis of which explicit predictions were made for DPE as well as for a similar two-gap process in which the proton dissociates. The latter, named SDD (for SD + DD), leads to SD events with a central rapidity gap within the diffraction dissociation cluster (see Fig. 7).

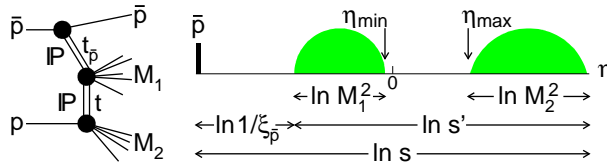


Figure 7: *SDD: Single+Double Diffraction [from Ref. 23)]*.

In 2003, CDF tested the renormalization model predictions for the above two-gap processes<sup>22, 23)</sup>, reporting agreement between data and model both in shape and normalization. In Fig. 8, data are compared with theory for one-gap to no-gap and two-gap to one-gap cross section ratios. While the one-gap/no-gap ratio is severely suppressed relative to the Regge theory prediction, the two-gap/one-gap ratios are relatively non-suppressed and equal to  $\approx \kappa$ . This result is expected in the renormalization model, since two-gap and one-gap cross sections are  $\propto \kappa^2$  and  $\propto \kappa$ , respectively, and gap probability factors are normalized to unity. In the next section we examine how the scaling features of multigap diffraction arise naturally in a QCD based framework for diffraction.

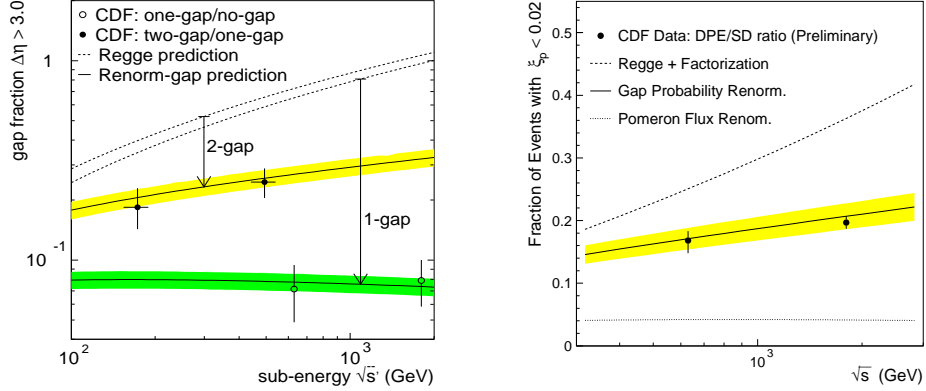


Figure 8: Comparison of ratios of cross sections with standard Regge theory and renormalization predictions: (left) ratios of SDD to SD (two-gap/one-gap) and SD to ND (one-gap/no-gap); (right) ratio of DPE to SD (two-gap/one-gap).

## 5 A parton model approach to diffraction

The form of the rise of total cross sections at high energies,  $\sim s^\epsilon$ , which in Regge theory requires a Pomeron trajectory with intercept  $\alpha(0) = 1 + \epsilon$ , is the form expected in a parton model approach, where cross sections are proportional to the number of available wee partons<sup>24</sup>). In terms of the rapidity region in which there is particle production<sup>2</sup>,  $\Delta\eta'$ , the total  $pp$  cross section is given by

$$\sigma_{pp}^{tot} = \sigma_0 \cdot e^{\epsilon\Delta\eta'} \quad (14)$$

Since from the optical theorem the total cross section is proportional to the imaginary part of the forward ( $t = 0$ ) elastic scattering amplitude, the full parton model amplitude may be written as

$$\text{Im } f^{\text{el}}(t, \Delta\eta) \sim e^{(\epsilon + \alpha' t)\Delta\eta} \quad (15)$$

where we have added to  $\epsilon$  the term  $\alpha'(t)$  as a parameterization of the  $t$ -dependence of the amplitude.

Based on this amplitude, the diffractive cross sections corresponding to the gap configurations we discussed above are expected to have the forms

$$\begin{aligned} \frac{d^2\sigma_{sd}}{dt d\Delta\eta} &= N_{gap}^{-1}(s) & F_p(t) \left\{ e^{[\epsilon + \alpha'(t)]\Delta\eta} \right\}^2 & \kappa \left[ \sigma_0 e^{\epsilon\Delta\eta'} \right] \\ \frac{d^3\sigma_{dd}}{dt d\Delta\eta d\eta_c} &= N_{gap}^{-1}(s) & \left\{ e^{[\epsilon + \alpha'(t)]\Delta\eta} \right\}^2 & \kappa \left[ \sigma_0 e^{\epsilon(\Sigma_i \Delta\eta'_i)} \right] \\ \frac{d^4\sigma_{sdd}}{dt_1 dt_2 d\Delta\eta d\eta_c} &= N_{gap}^{-1}(s) & F_p(t) \Pi_i \left\{ e^{[\epsilon + \alpha'(t_i)]\Delta\eta_i} \right\}^2 & \kappa^2 \left[ \sigma_0 e^{\epsilon(\Sigma_i \Delta\eta'_i)} \right] \\ \frac{d^4\sigma_{dpe}}{dt_1 dt_2 d\Delta\eta d\eta'_c} &= N_{gap}^{-1}(s) & \underbrace{\Pi_i \left\{ F_p(t_i) e^{[\epsilon + \alpha'(t_i)]\Delta\eta_i} \right\}^2}_{\text{gap probability factor}} & \underbrace{\kappa^2 \left[ \sigma_0 e^{\epsilon(\Delta\eta')} \right]}_{\sigma^{tot}(s')} \end{aligned} \quad (16)$$

where, as in Eq. (12), the (re)normalization factor  $N_{gap}(s)$  is the integral of the gap probability factor over all phase space in  $t_i$ ,  $\Delta\eta_i$  and the variables  $\eta_c$  and  $\eta'_c$ , which represent the center of the “floating” (not adjacent to a nucleon) rapidity gap in DD or SDD and the floating cluster in DPE, respectively. In

<sup>24</sup>We assume  $p_T = 1$  GeV so that  $\Delta y' = \Delta\eta'$ .



each case, the independent variables are the ones on the left hand side of the equation, but for pedagogical reason we use on the right hand side additional variables, which can be expressed in terms of the ones on the left.

A remarkable property of the above expressions is that they factorize into two term, one depending on the rapidity region(s) in which there is particle production and the other that consists of the rapidity gap(s). This is due to the exponential dependence on  $\Delta\eta$  of the elastic amplitude, which allows non-contiguous regions in rapidity to be added in the exponent. A consequence of this is that the (re)normalization factor is  $\sim s^{2\epsilon}$  in all cases, ensuring universal  $M^2$ -scaling.

These expressions may be understood as follows: (i) the term in square brackets represents the nucleon-nucleon total cross section at the reduced energy defined in Eq. (11); (ii) the factors  $\kappa$ , one for each gap, are the color factors required to enable rapidity gap formation; (iii) the gap probability factor is the amplitude squared of the elastic scattering between a diffractively dissociated and a surviving proton, in which case it contains the proton form factor,  $F_p(t)$ , or between two diffractively dissociated protons. Since the reduced energy cross section is properly normalized, the gap probability term is (re) normalized to unity using the  $N_{gap}^{-1}$  factor.

### 5.1 The parameters $\epsilon$ and $\kappa$

The parameters  $\epsilon$  and  $\kappa$  in Eqs. (16) have been experimentally found to be <sup>10, 11)</sup>

$$\begin{aligned} \text{experiment: } \epsilon &\equiv \alpha_{\mathbb{P}}(0) - 1 = 0.104 \pm 0.002 \pm 0.01 \text{ (syst)} \\ \kappa &\equiv \frac{g_{\mathbb{P}\mathbb{P}\mathbb{P}}}{\beta_{\mathbb{P}\mathbb{P}}} = 0.17 \pm 0.02 \text{ (syst)} \end{aligned} \quad (17)$$

where the systematic error assigned to  $\epsilon$  is a rough estimate by this author based on considering fits made to cross section data by various authors.

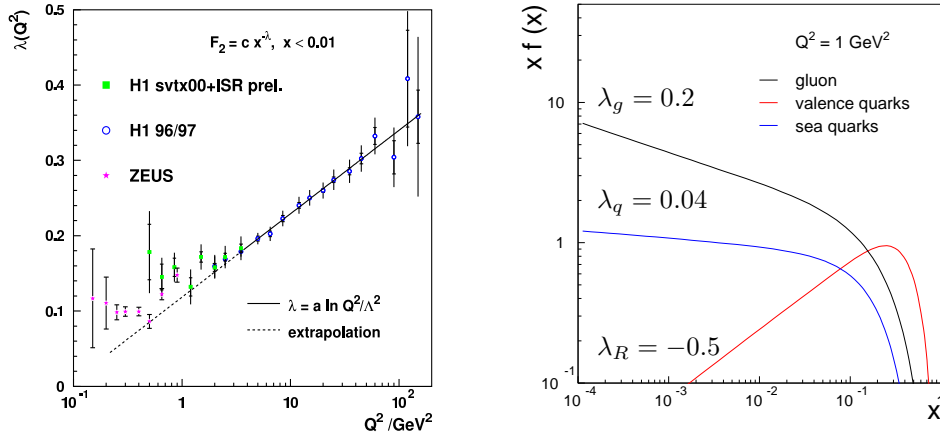


Figure 9: (left) The parameter  $\lambda$  versus  $Q^2$  of a fit to the structure function  $F_2(x, Q^2) \sim x^{-\lambda}$  in DIS at HERA <sup>25)</sup>; (right) CTEQ5L nucleon parton distribution functions for  $Q^2 = 1 \text{ GeV}^2$ .

Measurements of parton densities at HERA indicate that partonic structure in the nucleon may exist down to the hadron mass scale of  $Q^2 \approx 1 \text{ GeV}^2$ . This is seen in Fig. 9 (left), where the parameter  $\lambda(Q^2)$  of  $F_2(x, Q^2) \sim x^{-\lambda}$  decreases linearly with  $\ln Q^2$  down to  $Q^2 \approx 1 \text{ GeV}^2$ , flattening out and becoming consistent with  $\epsilon = 0.1$  only below  $Q^2 = 1 \text{ GeV}^2$ . We therefore assume partonic behavior in diffractive interactions and attempt to derive the parameters  $\epsilon$  and  $\kappa$  from the nucleon parton distribution functions (pdf's) at  $Q^2 = 1 \text{ GeV}^2$ , shown in Fig. 9 (right) for the CTEQ5L parameterization.

The region of interest to diffraction,  $x \leq 0.1$ , is dominated by sea gluons and quarks. In this region, a fit of the form  $xf(x) \sim x^{-\lambda}$  in Fig. 9 (right) yields  $\lambda_g \approx 0.2$  and  $\lambda_q \approx 0.04$  with relative

weights  $w_g \approx 0.75$  and  $w_q \approx 0.25$ <sup>3</sup>. Noting that the number of wee partons grows as  $\int_{1/s}^1 f(x)dx \sim s^\lambda$ , the Pomeron intercept may be obtained from the parameters  $\lambda_g$  and  $\lambda_q$ , appropriately weighted by a procedure involving gluon and quark color factors,

$$c_g = \frac{1}{N_c^2 - 1}, \quad c_q = \frac{1}{N_c} \quad (18)$$

Weighting places  $\epsilon$  in the range  $\lambda_q < \epsilon < \lambda_g$ , or  $0.04 < \epsilon < 0.2$ , which covers the experimental value of  $\epsilon = 0.104$ . The parameter  $\kappa$  is obtained from the  $g/q$  color factors and weights:

$$\kappa \approx c_g w_g + c_q w_q = 0.18 \quad (19)$$

This prediction is in remarkably good agreement with  $\kappa_{exp} = 0.17 \pm 0.02$ .

## 6 Soft diffraction summary

Using the (re)normalized gap probability model, which is based on a partonic description of diffraction, soft diffraction cross sections may be derived from the inclusive nucleon pdf's at  $Q^2 = 1 \text{ GeV}^2$ . No free parameters are required in the formulation of the  $t = 0$  differential cross sections: both the Pomeron intercept and the triple-Pomeron coupling (related to  $\kappa$ ) are derived from the underlying inclusive pdf's. Except for normalization, the procedure outlined reproduces the Regge theory predictions. Renormalization correctly predicts the data for all single and double gap processes studied by CDF, which include SD, DD, SDD and DPE. In all cases renormalization removes the explicit  $s^{2\epsilon}$  dependence from the cross section expressions in terms of  $M^2$ . This leads to  $M^2$ -scaling, which appears to be a basic property of diffraction at high energies. In the parton model,  $M^2$ -scaling is traced back to the power law behavior of the inclusive pdf's at low  $x$ . In summary, diffraction appears to be a low- $x$  interaction subject to color constraints.

In Ref. 9) it was pointed out that the Pomeron flux should be renormalized to unity only at high enough energies where it exceed unity. This remains true for central and multigap processes as well: renormalization of the Regge gap probability should be performed only for  $s$ -values for which  $P_{gap}(s) > 1$ . The parton model approach offers a simple explanation for this condition in terms of saturation effects.

## 7 Hard diffraction

Hard diffraction processes are defined as those in which there is a hard partonic scattering in addition to the diffractive rapidity gap signature. Events may have forward, central, or multiple rapidity gaps, as shown in Fig. (10) (*left*) for dijet production in  $\bar{p}p$  collisions at the Tevatron, and (*right*) for diffractive deep inelastic scattering (DIS) in  $ep$  collisions at HERA.

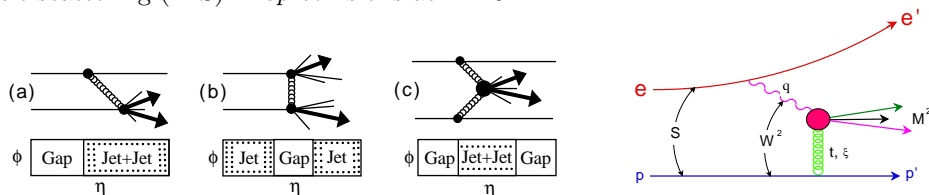


Figure 10: (*left*) Dijet production diagrams and event topologies for  $\bar{p}p$  (a) single diffraction (b) double diffraction and (c) double Pomeron exchange; (*right*) diffractive photon dissociation in  $ep$  collisions.

Results from Tevatron and HERA experiments have addressed several aspects of hard diffraction that are important for understanding its QCD nature. Process dependence of diffractive fractions and

<sup>3</sup>For valence quarks  $\lambda \approx -0.5$ ; this is relevant for Reggeon contributions, which are not considered here.

detailed comparisons of diffractive structure functions between Tevatron and HERA and within Tevatron data point to a picture in which the generic exchange mediating diffraction, generally referred to as Pomeron, appears to be a hard scale gluon or quark color-shielded by other gluons/quarks from the soft sector of the proton structure. Saturation effects in the soft sector, which are prominent at the Tevatron, lead to breakdown of QCD factorization between HERA and Tevatron, as well as within Tevatron data as a function of  $\sqrt{s}$ . Below, we briefly present some relevant results reported by the CDF Collaboration, compare Tevatron diffractive structure functions with predictions based on HERA data, and examine the applicability of the renormalized gap probability parton model approach to hard diffraction.

### 7.1 Process dependence

Diffractive fractions have been measured by CDF for  $W$  <sup>26)</sup>, dijet <sup>27)</sup>,  $b$ -quark <sup>28)</sup> and  $J/\psi$  <sup>29)</sup> production at  $\sqrt{s} = 1800$  GeV, as well as for events with a gap between jets at  $\sqrt{s} = 1800$  <sup>30)</sup> and  $\sqrt{s} = 630$  <sup>31)</sup> GeV. Table (7.1) presents the measured diffractive fractions within the indicated kinematic regions.

Table 1: *Diffractive fractions for forward and central gap processes at CDF*

Hard process	$\sqrt{s}$ (GeV)	$R = \frac{\text{DIFF}}{\text{TOTAL}}$ (%)	Kinematic region
$W(\rightarrow e\nu)+G$	1800	$1.15 \pm 0.55$	$E_T^e, \cancel{E}_T > 20$ GeV
Jet+Jet+G	1800	$0.75 \pm 0.1$	$E_T^{jet} > 20$ GeV, $\eta^{jet} > 1.8$
$b(\rightarrow e + X)+G$	1800	$0.62 \pm 0.25$	$ \eta^e  < 1.1, p_T^e > 9.5$ GeV
$J/\psi(\rightarrow \mu\mu)+G$	1800	$1.45 \pm 0.25$	$ \eta^\mu  < 0.6, p_T^\mu > 2$ GeV
Jet-G-Jet	1800	$1.13 \pm 0.16$	$E_T^{jet} > 20$ GeV, $\eta^{jet} > 1.8$
Jet-G-Jet	630	$2.7 \pm 0.9$	$E_T^{jet} > 8$ GeV, $\eta^{jet} > 1.8$

The diffractive fractions at  $\sqrt{s} = 1800$  GeV are approximately 1%. As the processes presented here have different sensitivities to the quark/gluon partonic component of the exchange, the measured fractions were used by CDF to extract the gluon fraction of the Pomeron <sup>28)</sup>. The result is compared below with the gluon fraction obtained by H1 from diffractive DIS at HERA <sup>32)</sup>:

$$\text{gluon fraction of } \mathbb{P}: \quad f_g^{\text{CDF}} = 0.54 \pm 0.15 \quad f_g^{\text{H1}} = 0.75 \pm 0.15 \quad (20)$$

The gluon fraction appears to be larger at HERA than at the Tevatron. Another interesting result is that the Jet-G-Jet fraction is larger at  $\sqrt{s} = 630$  than at 1800 GeV by a factor of  $2.3 \pm 0.9$ . These results will be revisited below when we present a parton model approach for hard diffraction, in which diffractive fractions are controlled by the underlying inclusive pdf's subject to renormalization and color constraints.

## 8 Factorization breakdown

The success of QCD in describing hard scattering processes rests on the factorization theorem, which allows hadronic cross sections to be expressed in terms of parton-level cross sections convoluted with uniquely defined hadron partonic densities. This success was shaken by the discovery that factorization breaks down in diffractive processes when comparing  $\bar{p}p$  collider results with results from diffractive DIS at HERA. The first comparison involved diffractive dijet production rates reported by UA8 <sup>5)</sup> and was made by this author in the paper proposing Pomeron flux renormalization mentioned in section 2. In the same paper, predictions were made for the Tevatron, which were later confirmed by experiment <sup>26, 27, 28, 29)</sup>. However, these experiments involved cross sections integrated over a range of  $x$ -Bjorken ( $x_{Bj}$  or  $x$ ) and thus provided no  $x$  or  $Q^2$  dependence of the factorization breakdown. Such information came later from CDF measurements <sup>33, 34)</sup> using a Roman Pot Spectrometer (RPS) to detect the leading antiproton in coincidence with two jets produced in the main detector,

$$\text{SD dijet production: } \quad \bar{p} + p \rightarrow \bar{p} + Jet_1 + Jet_2 + X \quad (21)$$

Obtaining  $x_{\bar{p}}$  from dijet production kinematics, CDF measured the ratio of rates of single diffractive (SD) to non-diffractive (ND) dijet production<sup>4</sup>, which in LO QCD approximately equals the ratio of the corresponding structure functions. From the ratio of rates, and after changing variables from  $x$  to  $\beta$ , where  $\beta \equiv x/\xi$  is the fractional momentum of the struck parton in the Pomeron, the diffractive structure function was obtained as a function of  $\beta$  and compared with predictions based on diffractive pdf's from HERA.

The structure function measured in dijet production has contributions from gluon and quark pdf's weighted by appropriate color factors:

$$F_{jj}(x) = x \left[ g(x) + \frac{4}{9}q(x) \right] \quad (22)$$

The CDF results for  $R(x)$ , the SD/ND ratio as a function of  $x$ , and for  $F_{jj}^D(\beta)$  versus  $\beta$  are presented in Fig. 11 (*left*) and (*right*), respectively.

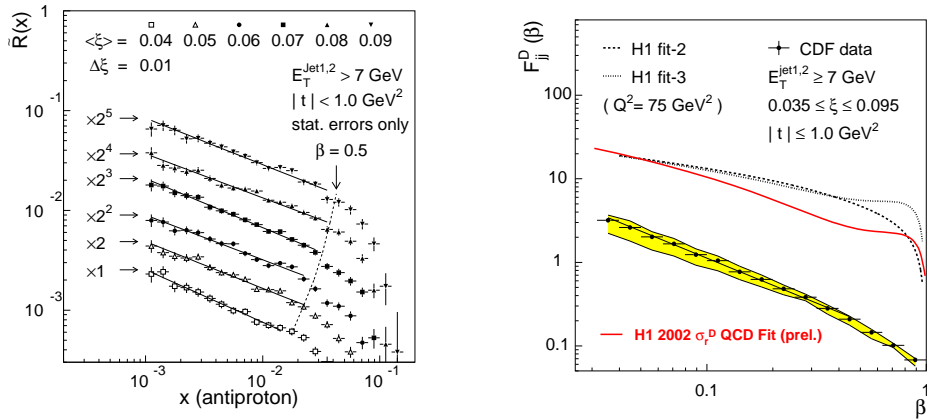


Figure 11: CDF diffractive dijet data at  $\sqrt{s} = 1800$  GeV: (*left*) Ratio of SD to ND dijet production rates versus  $x_{\bar{p}}$ ; (*right*) the CDF diffractive structure function versus  $\beta$  compared with predictions based on factorization and parton densities obtained by H1 from diffractive DIS at HERA<sup>32</sup>).

The data exhibit the following interesting features:

- Fig. 11 (*left*): In the region of  $0.035 < \xi < 0.095$  and  $\beta \equiv x/\xi < 0.5$ , the ratio of SD to ND rates (or structure functions) has no significant  $\xi$  dependence and decreases with increasing  $x$  as

$$R^{SD/ND}(x) = R_0 \cdot x^{-r}; \quad R_0 = (6.1 \pm 0.1) \times 10^{-3}, \quad r = 0.45 \pm 0.02 \quad (23)$$

- Fig. 11 (*right*): For  $\beta < 0.5$ ,  $F_{jj}^D(\beta)$  agrees in shape with the prediction from HERA but is suppressed by a factor of  $\approx 10$  (comparisons for  $\beta > 0.5$  should be avoided due to large systematic errors in the prediction).

The breakdown of factorization between Tevatron and HERA is generally attributed to additional partonic interactions that spoil the rapidity gap formed by Pomeron exchange. Under this scenario, factorization should also break down in diffractive  $\bar{p}p$  collisions at the Tevatron between different collision energies or between single and double gap processes.

### 8.1 $s$ -dependence of $F_{jj}^D$

Since the number of partons gets smaller at lower  $s$ ,  $F_{jj}^D$  should increase as  $s$  decreases. CDF measured the ratio of diffractive dijet production at  $\sqrt{s} = 630$  over 1800 GeV to be  $1.3 \pm 0.2(\text{stat})_{-0.3}^{+0.4}(\text{syst})$ <sup>34</sup>, but due to the large uncertainties no definitive conclusions can be drawn about the  $s$ -dependence of the factorization breakdown.

<sup>4</sup>As this ratio is  $< 1\%$ , we use ‘ND’ and ‘inclusive’ rates interchangeably throughout this paper.

## 8.2 $F_{jj}^D$ from double gap events

Factorization implies that the double-ratio  $D$  of dijet production in SD over ND events,  $R_{ND}^{SD}$ , to that of DPE over SD,  $R_{SD}^{DPE}$ , should be unity. However, since particles produced by additional partonic interactions spread throughout the entire available rapidity region, the two gaps in a DPE event either both survive or are simultaneously spoiled. Thus, factorization is expected to break down between the above two ratios, resulting in a deviation of  $D$  from unity. A CDF measurement of dijet production in DPE events yielded  $D = 0.19 \pm 0.07$  <sup>35)</sup>, confirming the expectation that the formation of the second gap is not, if at all, suppressed. This result is similar to the one discussed in section 4 for soft diffraction events.

## 9 Restoring factorization

For non-suppressed gaps, factorization should hold. This hypothesis was tested in a comparison <sup>5</sup> of the diffractive structure function measured on the proton side in events with a leading antiproton at the Tevatron with expectations from diffractive DIS at HERA. Results are shown in Fig. (12). The approximate agreement between Tevatron data and the expectation from HERA shows that factorization is largely restored for events that already have a rapidity gap.

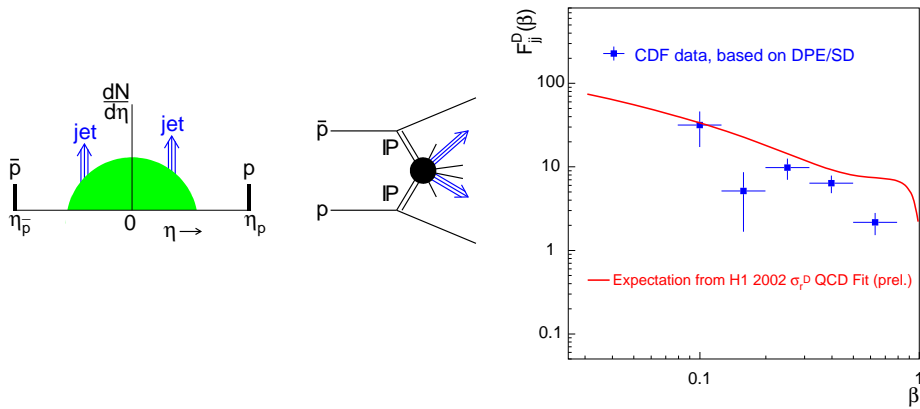


Figure 12: (left) Schematic representation of dijet production in DPE; (right) comparison of  $F_{jj}^D(\beta)$  of the proton in DPE events with expectations from H1 parton densities from diffractive DIS at HERA.

## 10 Rapidity gap survival probability

Hard diffraction calculations invariably involve estimates of the gap survival probability <sup>42)</sup> based on renormalization <sup>9)</sup>, “screening” <sup>38, 39)</sup>, or color neutralization by soft color exchanges <sup>40)</sup>. The non-perturbative nature of these estimates makes them model-dependent and difficult to obtain for all processes across the soft and hard diffractive sectors. The CDF two-gap results indicate that calculations for diffractive processes which already have a rapidity gap are largely free from gap survival considerations. Thus, multigap diffraction opens the way for QCD studies of diffraction without the complications arising from gap survival and will undoubtedly become the arena on which diffraction will be confronted by QCD at the Large Hadron Collider.

<sup>5</sup>The comparison was performed by the author and K. Hatakeyama using CDF published data <sup>35)</sup> and preliminary H1 diffractive parton densities <sup>32)</sup>.

## 11 Hard diffraction in a QCD framework

In this section we adapt the QCD approach of section 5 to diffractive DIS at HERA and diffractive dijet production at the Tevatron:

$$\begin{aligned} \text{HERA:} \quad & \gamma * +p \rightarrow p + Jet + X \\ \text{Tevatron:} \quad & \bar{p} + p \rightarrow +dijet + X \end{aligned}$$

The hard process may involve several color “emissions” from the surviving proton comprising a color singlet with vacuum quantum numbers. Two of the emissions have special importance: the one at  $x = x_{Bj}$  from the proton’s hard pdf at scale  $Q^2$ , which is responsible for the hard scattering, and the other at  $x = \xi$  from the soft pdf at  $Q^2 \approx 1 \text{ GeV}^2$ , which neutralizes the exchanged color and forms the rapidity gap. The diffractive structure function should then be <sup>36)</sup> the product of the inclusive structure function and the soft parton density at  $x = \xi$  [for simplicity, we do not include  $t$  dependence],

$$F^D(\xi, x, Q^2) \propto \frac{1}{\xi^{1+\epsilon}} \cdot F(x, Q^2) \sim \frac{1}{\xi^{1+\epsilon}} \cdot \frac{C(Q^2)}{(\beta\xi)^{\lambda(Q^2)}} \Rightarrow \frac{A_{\text{norm}}}{\xi^{1+\epsilon+\lambda}} \cdot c_{g,q} \frac{C}{\beta^\lambda} \quad (24)$$

where  $c_{g,q}$  are the color factors shown in Eq. (18),  $\lambda$  is the parameter of a power law fit to the relevant hard structure function in the region  $x < 1$  (see Fig. 13), and  $A_{\text{norm}}$  is a normalization factor.

$$x \cdot f(x) \propto x^{-\lambda}$$

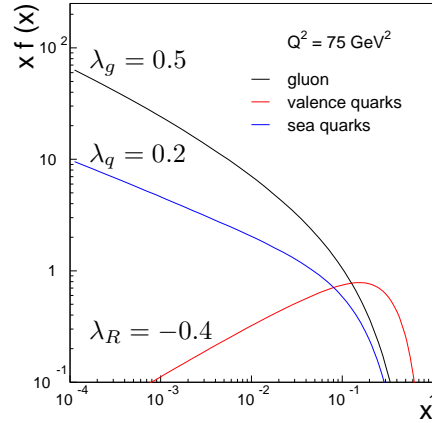


Figure 13: *CTEQ5L nucleon parton distribution functions for  $Q^2 = 75 \text{ GeV}^2$ . The parameters  $\lambda_{g,q,R}$  are the slopes of the gluon, sea quark, and valence quark distribution (‘R’ stands for Reggeon) in the region of  $x < 0.1$  where the power law behavior holds.*

### 11.1 Predictions for the diffractive structure function at HERA

At high  $Q^2$  at HERA, where factorization is expected to hold <sup>9, 41)</sup>,  $A_{\text{norm}}$  is simply the (constant) normalization factor of the soft pdf. This constant normalization leads to two important predictions:

- The Pomeron intercept in diffractive DIS (DDIS) is  $Q^2$ -dependent and equals the average of the soft and hard intercepts:

$$\begin{aligned} \alpha_{\mathbb{P}}^{DIS} &= 1 + \lambda(Q^2) \\ \alpha_{\mathbb{P}}^{DDIS} &= 1 + \frac{1}{2} [\epsilon + \lambda(Q^2)] \end{aligned} \quad (25)$$

- The ratio of DDIS to DIS structure functions at a given  $\xi$  is independent of  $x$  and  $Q^2$ :

$$R \left[ \frac{F^D(\xi, x, Q^2)}{F^{ND}(x, Q^2)} \right]_{\text{HERA}} = \frac{A_{\text{norm}} \cdot c_q}{\xi^{1+\epsilon}} = \frac{\text{constant}}{\xi^{1+\epsilon}} \quad (26)$$

HERA data are consistent with these predictions <sup>32)</sup>.

## 11.2 Predictions for the diffractive structure function at the Tevatron

At the Tevatron, where high soft parton densities lead to saturation,  $A_{\text{norm}}$  must be renormalized *ala* Eq. (6) by being replaced by

$$\text{Tevatron: } A_{\text{renorm}} = 1 / \int_{\xi_{\text{min}}}^{\xi=0.1} \propto \left( \frac{1}{\beta s} \right)^{\epsilon+\lambda} \quad (27)$$

where we have used  $\xi_{\text{min}} = x_{\text{min}}/\beta$  and  $x_{\text{min}} \propto 1/s$ . Thus, the diffractive structure function acquires a term  $\sim (1/\beta)^{\epsilon+\lambda}$ , and the diffractive to inclusive structure function ratio a term  $\sim (1/x)^{\epsilon+\lambda}$ . This prediction is confirmed by the CDF data on dijet production, where the  $x$ -dependence of the diffractive to inclusive ratio was measured to be  $\sim 1/x^{0.45}$  (see Eq. 23)<sup>6</sup>.

## 12 Summary and conclusion

We have reviewed experimental data on soft and hard diffraction, concentrating on aspects that point to the partonic nature of the exchange (Pomeron) responsible for rapidity gap formation.

In soft diffraction, the exponential dependence of total [elastic] cross sections on  $\Delta y'$  [ $\Delta y$ ], the rapidity region in which there is [there is not] particle production, allows differential diffractive cross sections to be factorized into two terms: one representing the total cross section at the reduced energy squared, defined by  $\ln(s'/s_0) = \sum_i \Delta y'_i$ , and the other depending on  $\sum_i \Delta y_i$  and interpreted as the gap formation probability. By (re)normalizing the latter to unity and multiplying by a color factor  $\kappa$  ( $\kappa^n$  for  $n$  gaps) derived from gluon and quark color factors weighted by the corresponding inclusive pdf's at  $Q^2 \approx 1 \text{ GeV}^2$ , cross sections for single, central, and multigap diffraction are obtained, which are in excellent agreement with experimental results. Prominent aspects of the data explained in this model are the  $M^2$ -scaling behavior and the independence on the number of gaps of the suppression of diffractive cross sections at high energies relative to Regge theory predictions.

In hard diffraction, the diffractive structure function is obtained by convoluting the inclusive  $F(Q^2, x)$  with the parton density at  $x = \xi$  at scale  $Q^2 \approx 1 \text{ GeV}^2$ , identifying the gap formation probability term, and (re)normalizing the latter to unity at the Tevatron. Aspects of the data explained by this approach are the rise of the Pomeron intercept with  $Q^2$  and the constant DDIS/DIS ratio versus  $x$  and  $Q^2$  at HERA, as well as the falling as  $\sim x^{-r}$  of the SD/ND ratio at the Tevatron. Also explained in this model is the factorization breakdown (and restoration for multigap diffraction!) between Tevatron diffractive structure functions and expectations from DDIS at HERA.

In conclusion, scaling and factorization aspects of the data have been phenomenologically interpreted in a parton model approach, in which diffraction is treated as a low  $x$  partonic interaction subject to color constraints.

## References

1. P.D.B. Collins, An Introduction to Regge Theory and High Energy Physics, Cambridge University Press (1977).
2. K. Goulianos, Diffractive Interactions of Hadrons at High Energies, Phys. Reports **101**, 171 (1983).
3. T.J. Chapin et al., Diffraction Dissociation of Photons on Hydrogen, Phys. Rev. D **31**, 17 (1985).
4. G. Ingelman (CERN) and P.E. Schlein, Jet Structure in High Mass Diffractive Scattering, Phys. Lett. B **152**, 256 (1985).
5. R. Bonino *et al.* (UA8 Collaboration), Evidence for Transverse Jets in High Mass Diffraction, Phys. Lett. B **211**, 239 (1988); A. Brandt et al., Phys. Lett. B **297**, 417 (1992).

---

<sup>6</sup>In calculating the value  $r$  of the  $\sim 1/x^r$  dependence, care should be taken to separately renormalize the sea gluon and sea quark contributions, and also consider the contribution of the valence quarks (Reggeon contributions).

6. F. Abe et al. (CDF Collaboration), Measurement of  $\bar{p}p$  Single Diffraction Dissociation at  $\sqrt{s} = 546$  and 1800 GeV, Phys. Rev D **50**, 5535 (1994).
7. K. Goulianos, Probing the Structure of the Pomeron at Hadron Colliders and at HERA, in: Proc. Les Rencontres de Physique de la Vallée d'Aoste, La Thuile, Aosta Valley, Italy, 5-11 Mar 1995.
8. K. Goulianos, Renormalized Diffractive Cross Sections at HERA and the Structure of the Pomeron, in: Proc. 7th Rencontres de Blois, Frontiers in Strong Interactions - 6th International Conference on Elastic and Diffractive Scattering, Blois, France, 20-24 Jun 1995; e-Print Archive: hep-ph/9512291.
9. K. Goulianos, Renormalization of Hadronic Diffraction and the Structure of the Pomeron, Phys. Lett. B **358**, 379 (1995); Erratum-*ib.* **363**, 268 (1995).
10. R.J.M. Covolan, J. Montanha, and K. Goulianos, A New Determination of the Soft Pomeron Intercept, Phys. Lett. B **389** (1996) 176.
11. K. Goulianos and J. Montanha, Factorization and Scaling in Hadronic Diffraction, Phys. Rev. D **59**, 114017 (1999).
12. K. Goulianos, From HERA to the Tevatron: A Scaling Law in Hard Diffraction, in: Proc. XXVII-th International Symposium on Multiparticle Dynamics, Frascati, Italy, 1997; Nucl. Phys. B (Proc. Suppl.) **71**, 368 (1999).
13. K. Goulianos, The Diffractive Structure Function at the Tevatron: CDF Results, in: Proc. Diffraction 2000, Cetraro, Italy, 2-7 September 2000; Nucl.Phys. Proc. Suppl. **99A**, 37 (2001); e-Print Archive: hep-ex/0011059.
14. K. Goulianos, Diffraction in Hadron-Hadron Interactions, in: Proc. Diffraction 2000, Cetraro, Italy, 2-7 September 2000; Nucl.Phys. Proc. Suppl. **99A**, 9 (2001); e-Print Archive: hep-ex/0011060.
15. K. Goulianos, Diffraction at the Tevatron in Perspective, in: Proc. NATO Advanced Research Workshop on Diffraction 2002, Alushta, Ukraine, 31 Aug - 6 Sep 2002; e-Print Archive: hep-ph/0306085.
16. K. Goulianos, Aspects of Diffraction at the Tevatron: Review and Phenomenological Interpretation of CDF Results on Diffraction, in: Proc. 8th Conference on the Intersections of Particle and Nuclear Physics (CIPANP 2003), New York, New York, 19-24 May 2003; AIP Conf. Proc. **698**, 110-114 (2004); e-Print Archive: hep-ph/0308183.
17. K. Goulianos, Diffraction: Results and Conclusion, in: Proc. Lafex International School of High Energy Physics, Rio de Janeiro, Brazil, February 16-20 1998 (ed. Andrew Brandt, Hélio da Motta, and Alberto Santoro); e-Print Archive: hep-ph/9806384.
18. T. Affolder et al. (CDF Collaboration), Double Diffraction Dissociation at the Fermilab Tevatron Collider, Phys. Rev Lett. **87**, 141802 (2001).
19. K. Goulianos, Beyond the Conventional Pomeron, High Energy QCD: Beyond the Pomeron, Brookhaven national Laboratory, Upton, Long Island, NY, 21-25 May 2001, in: Proc. of RIKEN BNL Research Center Workshop, Vol. 34, p. 113.
20. K. Goulianos, The Nuts and Bolts of Diffraction, in: Proc. Snowmass 2001, Study on the Future of particle Physics, Snowmass, CO, USA, July 2001 (ed. Norman Graf, eConf C010630:P502, 2001); e-print Archive: hep-ph/0110240.
21. K. Goulianos, Diffraction in QCD, in: Corfu Summer Institute on Elementary Particle Physics, Corfu, Greece, 31 Aug - 20 Sep 2001; e-print Archive: hep-ph/0203141 Mar 2002.
22. D. Acosta *et al.* (CDF Collaboration), Inclusive double Pomeron exchange at the Fermilab Tevatron  $\bar{p}p$  collider, submitted to Phys. Rev. Lett. (2003).
23. D. Acosta et al. (CDF Collaboration), Central Pseudorapidity Gaps in Events with a Leading Antiproton at the Fermilab Tevatron  $\bar{p}p$  Collider, Phys. Rev Lett. **91**, 011802 (2003).



24. E. Levin, An Introduction to Pomerons, Preprint DESY 98-120.
25. A. Petrukhin (H1 Collaboration), Measurement of the Inclusive DIS Cross Section at Low  $Q^2$  and High  $x$  Using Events with Initial State Radiation, presented at DIS2004, 14-18 April 2004, Slovakia.
26. F. Abe *et al.* (CDF Collaboration), Observation of Diffractive  $W$  Boson Production at the Fermilab Tevatron, Phys. Rev. Lett. **78**, 2698 (1997).
27. Abe, F. *et al.* (CDF Collaboration), Measurement of Diffractive Dijet production at the Fermilab Tevatron, Phys. Rev. Lett. **79**, 2636 (1997).
28. Affolder, T. *et al.* (CDF Collaboration), Observation of Diffractive  $b$ -quark Production at the Fermilab Tevatron, Phys. Rev. Lett. **84**, 232 (2000).
29. Affolder, T. *et al.* (CDF Collaboration), Observation of Diffractive  $J/\psi$  Production at the Fermilab Tevatron, Phys. Rev. Lett. **87**, 241802 (2001).
30. Abe, F. *et al.* (CDF Collaboration), Dijet Production by Color-Singlet Exchange at the Fermilab Tevatron, Phys. Rev. Lett. **80**, 1156 (1998).
31. Abe, F. *et al.* (CDF Collaboration), Events with a Rapidity Gap between Jets in  $\bar{p}p$  Collisions at  $\sqrt{s} = 630$  GeV, Phys. Rev. Lett. **81**, 5278 (1998).
32. F.P. Schilling (H1 Collaboration), Measurement and NLO DGLAP QCD Interpretation of Diffractive Deep-Inelastic Scattering at HERA, in: Paper submitted to 31st International Conference on High Energy Physics, ICHEP02, Amsterdam, The Netherlands, Jul. 24–31, 2001 (abstract 980).
33. Affolder, T. *et al.* (CDF Collaboration), Diffractive Dijets with a Leading Antiproton in  $\bar{p}p$  Collisions at  $\sqrt{s} = 1800$  GeV, Phys. Rev. Lett. **84**, 5083 (2000).
34. Acosta, A. *et al.* (CDF Collaboration), Diffractive Dijet Production at  $\sqrt{s}=630$  and 1800 GeV at the Fermilab Tevatron, Phys. Rev. Lett. **88**, 151802 (2002)
35. Affolder, T. *et al.* (CDF Collaboration), Dijet Production by Double Pomeron Exchange at the Fermilab Tevatron, Phys. Rev. Lett. **85**, 4215 (2000).
36. K. Goulios, Pomeron: Beyond the Standard Approach, in: Proc. 29th International Symposium on Multiparticle Dynamics (ISMD 99), Providence, Rhode Island, 8-13 Aug 1999 (Providence 1999, QCD and multiparticle production, pp. 298-303); e-Print Archive: hep-ph/9911210.
37. K. Goulios, Diffraction: a New Approach, in: Proc. UK Phenomenology Workshop on Collider Physics, Durham, England, 19-24 Sep 1999; J. Phys. G **26**, 716 (2000); e-print Archive: hep-ph/0001092 Jan 2000.
38. E. Gotsman, E. Levin, and E. Maor, The Survival Probability of Large Rapidity Gaps in a Three Channel Model, Phys. Rev D **60**, 094011 (1999).
39. A.B. Kaidalov, V.A. Khoze, A.D. martin, and M.G. Ryskin, Probabilities of Rapidity-Gaps in High Energy Interactions, Eur. Phys. J. C **21**, 521 (2001) and references therein.
40. R. Enberg, G. Ingelman, and N. Timneanu, Rapidity Gaps at HERA and the Tevatron from Soft Color Exchanges, J. Phys. G **21**, 712 (2000); *ibid.* Soft Color Interactions and Diffractive Hard Scattering at the Tevatron, Phys. Rev. D **64**, 114015 (2001).
41. J. Collins, Factorization in Hard Diffraction, J. Phys. G **28**, 1069 (2002); arXiv:hep-ph/0107252.
42. J.D. Bjorken, Rapidity Gaps and Jets as a New Signature in Very High-Energy Hadron-Hadron Collisions, Phys. Rev. D **47**, 101 (1993).